


 Cite this: *RSC Adv.*, 2021, **11**, 10582

Cell cycle arrest of human bronchial epithelial cells modulated by differences in chemical components of particulate matter†

 Zheng Yang,^{‡a} Qingyang Liu,^{‡c} Yanju Liu,^{*ab} Xuekui Qi^b and Xinxin Wang^b

There is increasing interest in understanding the role of airborne chemical components in modulating the cell cycle of human bronchial epithelial (HBE) cells that is associated with burden of cardiopulmonary disease. To address this need, our study collected ambient PM₁₀ (particles with aerodynamic diameter less than or equal to 10 μm) and PM_{2.5} (particles with aerodynamic diameter less than or equal to 2.5 μm) across four sampling sites in Beijing during the year of 2015. Chemical components including organic carbon (OC), elemental carbon (EC), polycyclic aromatic hydrocarbons (PAHs), metals and water soluble ions were determined. Spearman's rank-order correlation was performed to examine the associations between chemical components in ambient particles and cell cycle distributions with *p*-values adjusted by Bonferroni methodology. Our results demonstrated the significant associations between certain chemical compositions (*i.e.*, PAHs, EC, As and Ni) and percentages of HBE cells in G0/G1 and G1/G2 phases, respectively. Our results highlighted the need to reduce the specific toxins (*e.g.*, PAHs, EC, As and Ni) from ambient particles to protect cardiopulmonary health associated with air pollution. Future study may focus on illustrating the mechanism of certain chemical compositions in altering the cell cycle in HBE cells.

Received 16th December 2020

Accepted 5th March 2021

DOI: 10.1039/d0ra10563e

rsc.li/rsc-advances

Introduction

Ambient particulate matter (PM) is listed as carcinogens to humans by the International Agency for Research on Cancer (IARC).¹ It is estimated that more than 4 million premature deaths were associated with long-term exposure to atmospheric PM_{2.5} in 2015 globally.² Ambient fine particle could enter into the human body and increase incidences of cardiopulmonary diseases.^{3,4} Studies on biological mechanisms that illustrated PM exposure to adverse health outcomes showed that systemic inflammation may be a key mediator.^{5–7} Though ambient PM is a complex of chemical components including OC, EC, metals and water soluble ions that emit from diverse sources,^{8–10} adverse health effects resulted from PM were found to be highly associated with certain chemical components rather than total mass.^{11,12} Several *in vivo* biological studies have shown certain chemical components including PAHs and metals from various

sources could cause the increased levels of pro-inflammatory cytokines in circulating blood.^{5,13}

Recently, some *in vitro* studies showed that PM may inhibit cell proliferation by cell cycle arrest.^{14–16} Cell proliferation plays an important role in maintaining the normal morphology and function of tissues.¹⁷ Under pathological conditions, the disorder in cell cycle could lead to further destruction of tissue cells and aggravation of inflammatory reaction.¹⁸ Cell cycle alterations lead to influence structural dysfunction of various proteins by blocking DNA integrity checkpoint at G0/G1 or G1/G2 phases.¹⁹ The maladjustment in cell cycle resulted from exposures to PM, in the long run, could also be progressive to carcinogenesis.^{19,20} Few studies illustrated which chemical components of PM were key factors for altering cell cycle. Fu *et al.*¹⁹ observed the increased levels of urinary biomarkers of PAHs exposure (8-hydroxy-2'-deoxyguanosin) were associated with cell cycle arrest in venous blood among Chinese coke oven workers. Although the study presented the associations between chemical components (*e.g.*, PAHs) and cell cycle arrest, it lacks the evidence that cell cycle arrest is linked to PAHs from ambient particle directly. Thus, further studies are required to investigate and clarify which chemical components from airborne PM may result in cell cycle arrest.

Air pollution including haze and dust storm occurs frequently and intensively in most areas of China, which cause tremendous health issues and economic costs.⁴ Since January 2015, new Environmental Protection Law was issued by Chinese

^aBeijing Milu Ecological Research Center, Beijing, 100076, China. E-mail: liuyanju@hotmail.com

^bBeijing Center for Physical and Chemical Analysis, Beijing, 100089, China

^cCollege of Biology and the Environment, Nanjing Forestry University, Nanjing, Jiangsu Province 210037, China

† Electronic supplementary information (ESI) available. See DOI: 10.1039/d0ra10563e

‡ The two authors contribute equally.



Ministry of Environmental Protection.²¹ Levels of air pollution are classified as four groups to publicize widely in China, which are red, orange, yellow and blue alerts, respectively.²² This implemented action could aid the citizens to prevent the health risks associated with air pollution.²² According to the definition of haze weather in China (QX/T 113-2010),⁵ haze is defined as the weather with visibility lower than 10 km, relative humidity lower than 95% and PM_{2.5} mass greater than 75 $\mu\text{g m}^{-3}$. Floating dust weather in China is defined as visibility lower than 10 km, which is impacted by the mineral particles with the transport of the strong surface winds from arid areas in Asian continent.⁸ Haze and floating dust weather both frequently occurred in Beijing, which contributed to high PM₁₀ and PM_{2.5} pollution days and increased incidences of cardiovascular disease.^{6,8,23} Prior studies on chemical components of PM_{2.5} collected during haze periods in Beijing indicated that secondary ions (*i.e.*, NO₃²⁻, SO₄²⁻, NH₄⁺) and organic compounds dominated the mass loadings of PM_{2.5}.²³ In contrast, crystal metals including Si, Al, Fe and Ca were the main chemical components of PM_{2.5} on floating dust samples in Beijing.^{6,7}

Till now, limited study was conducted to illustrate which chemical components of ambient particles inhibit cell proliferation *via* cell cycle arrest. Our study aims to examine if cell cycle arrest resulted from the exposures to PM are related to the chemicals across diverse PM sample types. To test this hypothesis, we collected ambient PM samples (PM₁₀ and PM_{2.5}) during haze and floating dust days at four sampling sites in Beijing and determined chemical components including PAHs, OC, EC, ions, metals. We measured cell survival rate and cell cycle distribution in human bronchial epithelial cells (HBE) after HBE cells were exposed to water extracts of PM for 24 h. Our study aims to investigate which chemical compounds of airborne PM samples from emission sources are the main

mediators for altering cell cycles. The results may aid local government to frame relevant policies in reductions of certain airborne chemical compounds responsible for cardiopulmonary disease as new Environmental Protection Law launched.

Method

Collections of PM samples

Two parallel PM₁₀ and PM_{2.5} samplers were placed at four sites in Beijing in spring and winter of 2015 (Fig. 1). S₁ site (116.34E, 39.49N) is a rural site in southern Beijing. S₂ site (116.3E, 39.95N) is an urban site in northeastern Beijing. S₃ site (116.36E, 39.99N) is an urban site in northern Beijing. S₄ site (116.10E, 40.13N) is a rural site in northeastern Beijing (Fig. 1). At S₁ site, PM₁₀ and PM_{2.5} samples were collected on March 28, 29 and April 17, 2015. For site S₂, PM₁₀ and PM_{2.5} samples were collected on April, 9 and April 15, 2015. At site S₃, PM₁₀ and PM_{2.5} samples were collected on March, 16 and March 17, 2015. The collections of PM₁₀ and PM_{2.5} at site S₄ were carried out on November 12, 13 and 14, 2015 (Table S1[†]). Because the major sources and chemical compositions responsible for PM pollution in Beijing varied greatly across seasons and sites,²⁴ the selections of representative PM₁₀ and PM_{2.5} samples during air pollution days across diverse sites and seasons in Beijing are more comprehensive for illustrating effects of PM components on cell proliferation in HBE cells. The PM₁₀ and PM_{2.5} samples were collected on 90 mm quartz fiber membrane (Whatman, UK) with the use of a medium flow PM sampler (Qingdao Laoying, 100 L min⁻¹). Each sample was collected for 24 hours. Prior to sampling, the quartz fiber membrane was heated at 550 °C for 4 h to remove organic residues.⁶ After sampling, the filter was sealed and stored in a refrigerator at -18 °C before shipped to the laboratory for chemical analysis.⁵ Two field blanks (PM₁₀ and PM_{2.5}) at each sample site were collected

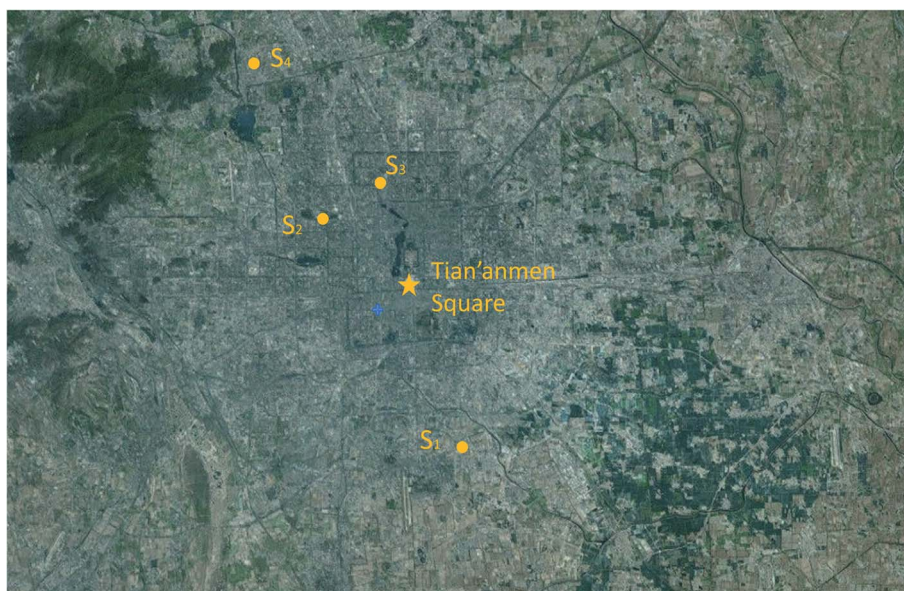


Fig. 1 The map of sampling locations. S₁, Milu Park (116.34E, 39.49N); S₂, Beike (116.31E, 39.95N); S₃, Huayuan (116.36E, 39.99N); S₄, Changping rural site (116.10E, 40.13N). Image was from Google Map. Map data: GS (2011). Imagery: CNES/Astrium, Cnes/Spot Image, Digital Globe, Landsat.



during the sampling period by loading filters into the samplers without starting the instrument.

Chemical components in PM samples

Filters were weighed in a climate-controlled room (25 °C, 40%) using a microbalance (0.01 mg, Sartorius, Germany). The mass concentrations of PM₁₀ and PM_{2.5} were estimated using the mass differences between filters before and after sampling divided by sampling volume. The calculated mass concentrations of PM on each day were corrected by subtracting mass concentrations of field blank. After gravimetric mass measurement, each filter was divided into quarter sections. Each quarter is ~15 cm² in area.

One quarter of quartz fiber filter samples was extracted with 20 mL de-ionized water for 30 min with the use of table shaker. Then, the extracts were filtered through 0.45 μm pore syringe filters to remove insoluble substances before chemical analysis. Water soluble ions (Cl⁻, NO₃⁻, SO₄²⁻, Na⁺, NH₄⁺, Ca²⁺, K⁺ and Mg²⁺) in extracts were determined by and ICS 2000 ion chromatography (Thermo, USA).⁸ The filters spiked with certain concentrations (10 μg L⁻¹) of mixed ions were performed in the same procedure to examine the extraction recoveries. The

recoveries for measuring water soluble ions in PM samples were in the range of 90–98%.

0.518 cm² of quartz filters were used for OC and EC measurements. The OC and EC were measured by a DRI-2001AOC/EC Analyzer (Model 2001 A, Desert Research Institute) with a thermal-optical transmission protocol.⁸ The detection limits for OC and EC measurements were 0.2 μg m⁻³.

A half of quartz filter was chosen for measure seven metals (As, Cr, Cu, Ni, Pb, Mn and Zn) in PM_{2.5} and PM₁₀ samples by X-ray fluorescence analyzer (Mesa-50, Horiba company, Japan).²⁵ X-ray fluorescence spectroscopy is a method for elemental analysis with high stability and without pretreatment.²⁵ The detection limits for seven metals (Cr, Cu, Ni, Pb, Mn and Zn) varied from 0.02 to 0.05 μg m⁻³.

A quarter of quartz filter was ultrasonicated with dichloromethane and methanol (3/1, v/v) for three times in 45 min. Then the extract was concentrated to about 0.5 mL for chemical analysis. PAHs including naphthalene (Nap, 2 ring, C₁₀H₈), acenaphthylene (AcPy, 3 ring, C₁₂H₈), acenaphthene (Acp, 3 ring, C₁₂H₁₀), fluorene (Flu, 3 ring, C₁₃H₁₀), phenanthrene (PA, 3 ring, C₁₄H₁₀), anthracene (Ant, 3 ring, C₁₄H₁₀), pyrene (Pyr, 4 ring, C₁₆H₁₀), fluoranthene (FL, 4 ring, C₁₆H₁₀), chrysene (CHR, 4 ring, C₁₈H₁₂), benzo(a)anthracene (BaA, 4 ring, C₁₈H₁₂), benzo(k)fluoranthene (BkF, 5 ring, C₂₀H₁₂), benzo(b)fluoranthene

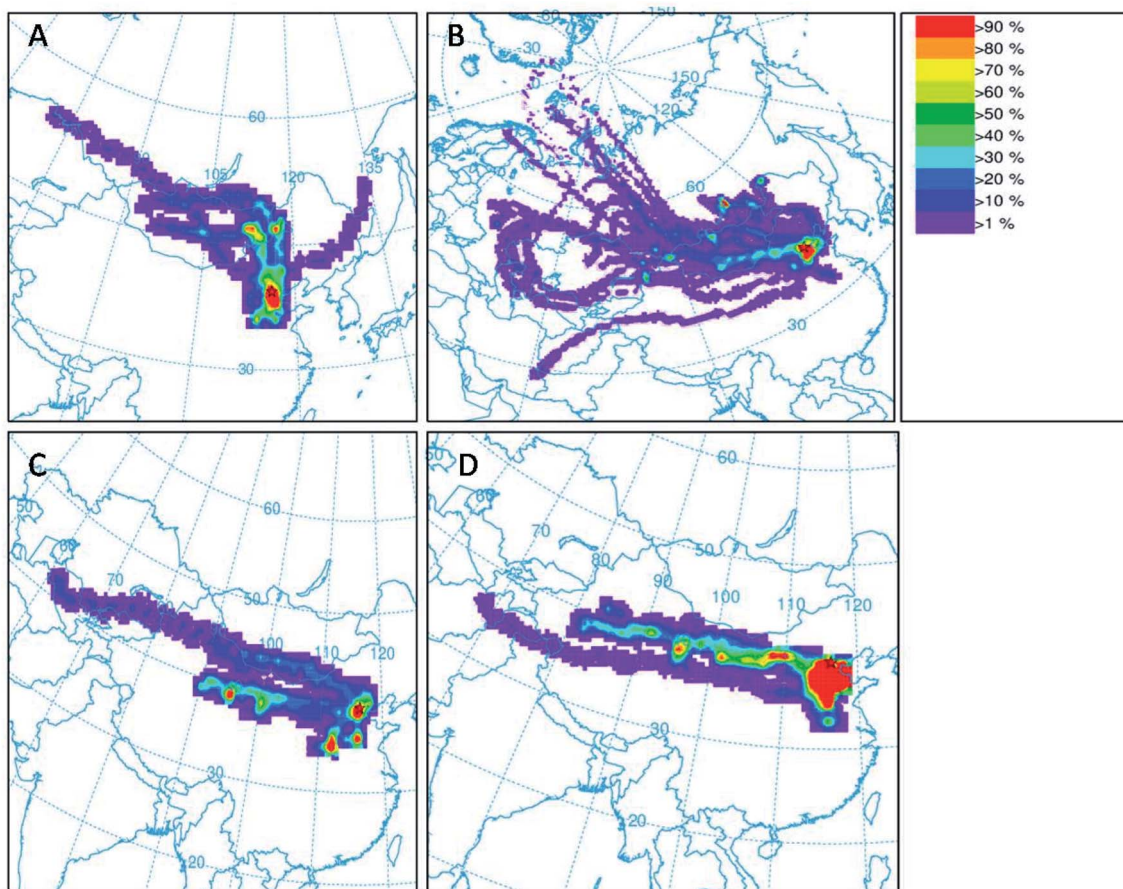


Fig. 2 (A) Frequencies of air trajectories were obtained from 27 to 29 March (A), from 9 to 17 April (B), 15 to 17 March (C) and from 11 to 14 November (D).



(BbF, 5 ring, C₂₀H₁₂), benzo(*a*)pyrene (BaP, 5 ring, C₂₀H₁₂), dibenzo(*a,h*)anthracene (DBA, 5 ring, C₂₂H₁₄), indeno(1,2,3-*cd*)pyrene (IND, 6 ring, C₂₂H₁₂), benzo(*g,h,i*)perylene (BghiP, 6 ring, C₂₂H₁₂) were analyzed using gas chromatography (Agilent 5890, Agilent Technologies, USA) and a mass spectrometer (Agilent 5975, Agilent Technologies, USA) with an electron impact ion (EI) source.⁵ The extraction recoveries were estimated with the filter spiked with 30 μL isotopically-labeled PAHs, including acenaphthylene-d₁₀, chrysene-d₁₂, perylene-d₁₂ and phenanthrene-d₁₀. The extraction recoveries ranged from 85–92% and the detection limits for PAHs were in the range of 0.01–0.03 $\mu\text{g m}^{-3}$, respectively. All the samples for chemical component analyses were blank-corrected.

Cell cultures

We purchased human bronchial epithelial (HBE) cells from Shanghai Institute of Cell Biology, Chinese Academy of Sciences. HBE cells were cultured with Dulbecco's Modified Eagle Medium (MEM) vitamin solution mixed with a solution of 10% fetal bovine serum, 100 U mL⁻¹ penicillin, and 100 mg mL⁻¹ streptomycin in 5% CO₂ at 37 °C incubators. Cells were harvested for subculture at a ratio of 1 : 3 every 2 days.¹⁸

MTT assay

Standard 3-(4,5-dimethylthiazole)-2,5-diphenyltetrazoliumbromide (MTT) assay procedures were obtained to measure cell survival rates after HBE cells were exposed to water extracts of PM for 24 h.²⁶ Briefly, a quarter of each filter sample was mixed with de-ionized water on a shaker table for about 2 h at 37 °C in a darkroom. Then, the water extracts were filtered through a 0.22 mm PTFE syringe filter for further exposure. We introduced the water extracts of PM samples to cultured HBE cells and then assessed survival rates of HBE cells after 24 h. The exposure concentrations for mass normalized PM water extracts concentrated at 1 $\mu\text{g mL}^{-1}$ were prepared by adding an aliquot of the 10 \times concentrated MEM vitamin solution.

Cells were placed in 96-well microassay culture plates with a density of 1 $\times 10^4$ cells per well and cultured for ~ 12 h at 37 °C in a 5% CO₂ incubator. Then, the cell culture medium was removed and replaced with the exposure solutions for PM water extracts. After 24 h exposure, 20 μL of MTT dye solution concentrated at 5 mg mL⁻¹ was added into each cell. After 4 h, a 100 μL buffer solution of *N,N*-dimethylformamide (50%) and sodium dodecyl sulfate (20%) was introduced into each cell for

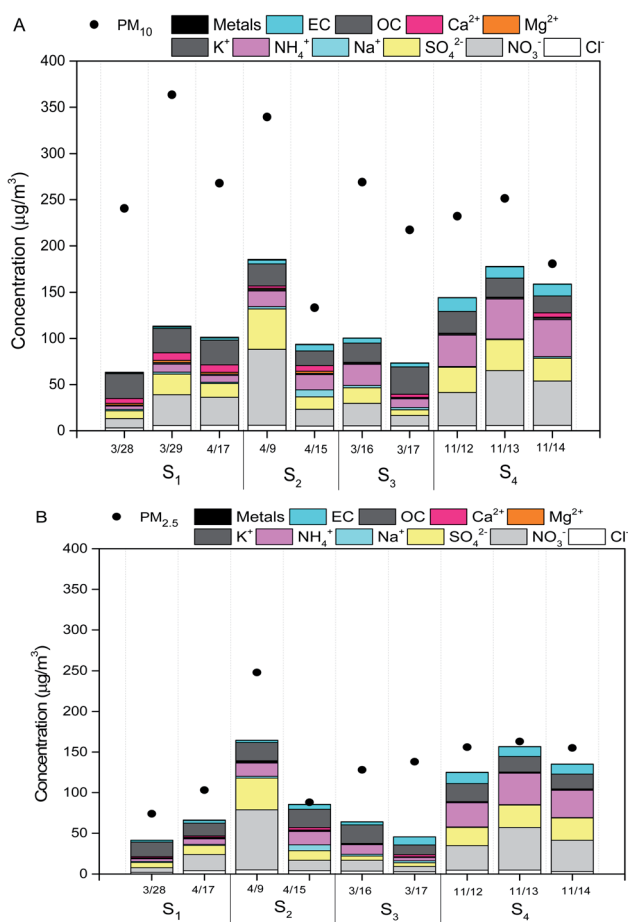


Fig. 3 Variations of PM₁₀ (A) and PM_{2.5} (B) mass and major chemical components at four different sampling sites in Beijing during the year of 2015. Metals refers to the sum of As, Cr, Cu, Ni, Pb, Mn and Ni.

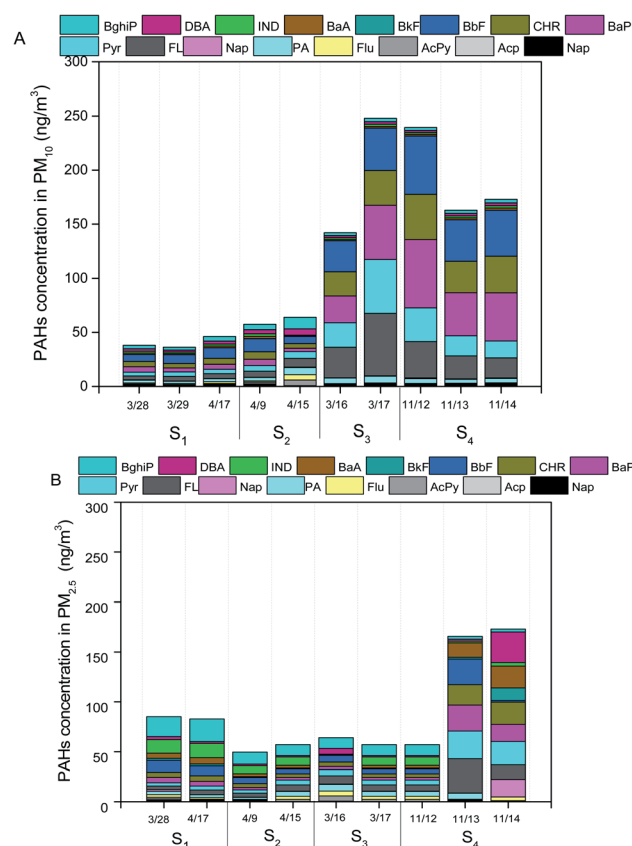


Fig. 4 Concentrations of PAHs in PM₁₀ (A) and PM_{2.5} (B) at four different sampling sites in Beijing during the year of 2015. Naphthalene (Nap), acenaphthylene (AcPy), acenaphthene (Acp), fluorene (Flu), phenanthrene (PA), anthracene (Ant), pyrene (Pyr), fluoranthene (FL), chrysene (CHR), benzo(*a*)anthracene (BaA), benzo(*k*)fluoranthene (BkF), benzo(*b*)fluoranthene (BbF), benzo(*a*)pyrene (BaP), dibenzo(*a,h*)anthracene (DBA), indeno(1,2,3-*cd*)pyrene (IND), benzo(*g,h,i*)perylene (BghiP).



solubilizing MTT formazan. The optical density of each cell was analyzed using a microplate spectrophotometer at a wavelength of 490 nm. A negative control experiment (*e.g.*, without the extracted PM solution) was performed under the same conditions at the same time. Survival rates of HBE cells were determined by plotting the percentage viability *versus* concentration relative to the control. Each experiment was repeated for three times and the mean values were used for statistical analysis.

Cell cycle arrest assay

We used propidium iodide staining method to perform cell cycle analysis.^{19,27} HBE cells were collected after exposure to mass normalized water extracts of PM ($1 \mu\text{g mL}^{-1}$) for 24 h. Then, cells were centrifuged at 1000g for about 5 min and fixed with 70% ethanol at -20°C . After that, $30 \mu\text{g mL}^{-1}$ DNase-free was added into the cells and incubated for 10 min at 37°C , and then the exposed cells were mixed with $80 \mu\text{L}$ of propidium iodide concentrated at $150 \mu\text{g mL}^{-1}$ for 15 min at 4°C in a darkroom. Cell cycle analysis was determined by flow cytometry (BD FAC Canto II, USA), which acquires 20 000 events for ModFit software analysis. We carried out a negative control

experiment (*e.g.*, without the extracted PM solution) under the same conditions simultaneously. We performed each experiment for three times and chose the averaged values for statistical analysis.

Air mass back trajectories

Air mass back trajectories were estimated with the aid of the National Oceanic and Atmospheric Administration (NOAA)'s ARL HYSPLIT 4.0 model. The corresponding meteorological data were obtained from the Global Data Assimilation System (GDAS).²⁸ Frequencies of back trajectories calculated at the 500 m level were estimated for every 6 h interval during the sampling periods.

Statistical analysis

Summary statistics for data on cell survival rate and cell cycle arrest are shown as the mean and standard deviation for each day using the results from at least three independent experiments conducted with the ambient PM sample. We used the Wilcoxon rank-sum test to compare the mean differences in chemical components, cell survival rate and cell cycle arrest

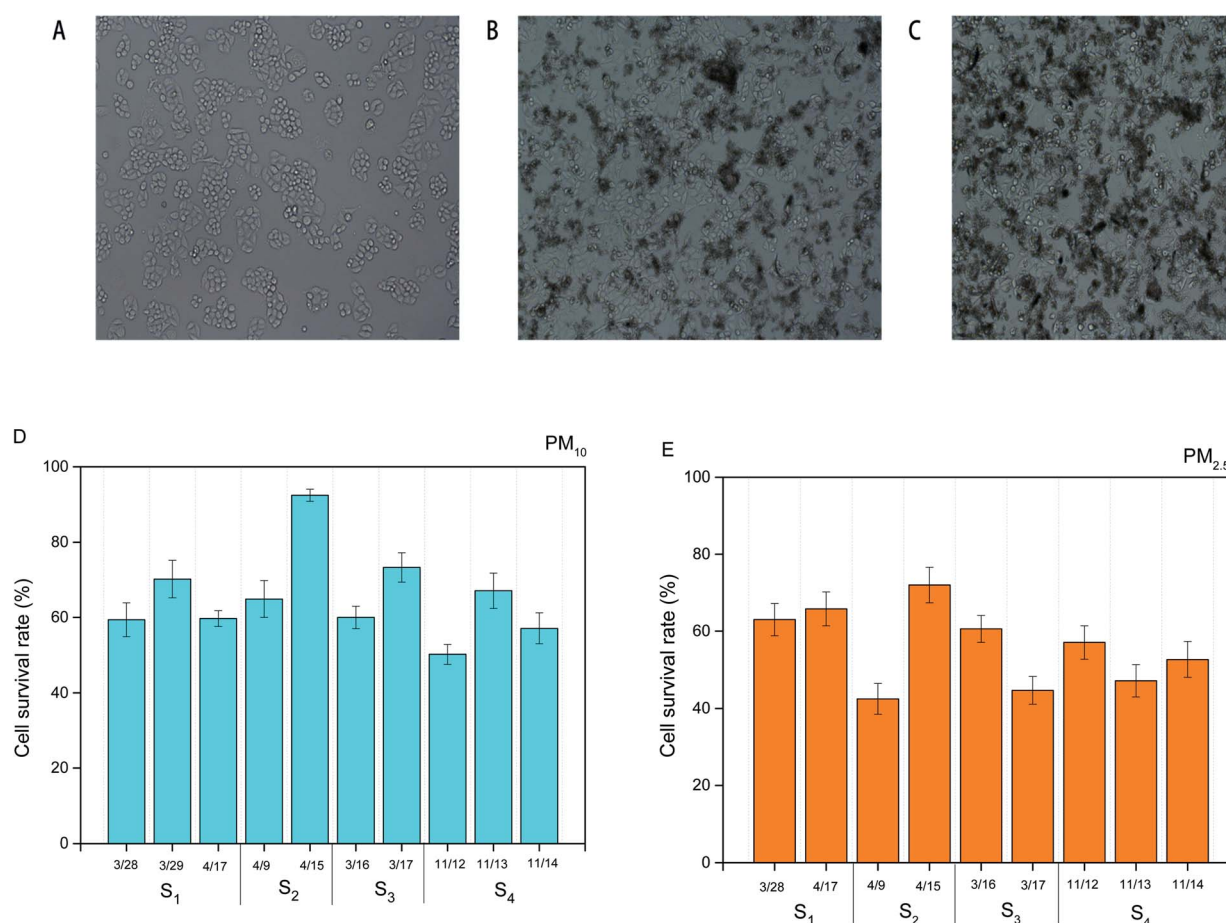


Fig. 5 Human bronchial epithelial cells treated with mass normalized PM water extracts ($1 \mu\text{g mL}^{-1}$). (A) Cells without treatment. (B) Cells with PM₁₀ water extracts ($1 \mu\text{g mL}^{-1}$). (C) Cells with PM_{2.5} water extracts ($1 \mu\text{g mL}^{-1}$). Survival rate in human bronchial epithelial cells with mass normalized PM water extracts ($1 \mu\text{g mL}^{-1}$) after 24 h exposure. (D) Cells with PM₁₀ water extracts ($1 \mu\text{g mL}^{-1}$), (E) cells with PM_{2.5} water extracts ($1 \mu\text{g mL}^{-1}$). Summary statistics for data on cell survival rate and cell cycle arrest are shown as the mean and standard deviation for each day using the results from at least three independent experiments conducted with the ambient PM sample.



across sampling sites because the dataset is non-normal distribution from the assessment of Shapiro–Wilk test. We performed a *post hoc* test using Bonferroni methodology to adjust *p*-values for pairwise comparisons.²⁹

We assessed the associations between PM mass and chemical components and cell survival rate and cell cycle distribution using univariate correction analyses. Spearman's rank-order correlation analyses were adopted in this study the dataset is non-normal distribution. Since correlations in data are related to ordering, several data may yield “significant” results by chance.²⁹ Therefore, *p*-values are needed to be adjusted using Bonferroni methodology to compensate for this problem.²⁹ Significant correlation were considered as strong for $\rho > 0.8$, adjusted *p* value < 0.05 , and moderate for $0.6 < \rho < 0.8$, adjusted *p* value < 0.05 , which are criteria that have been used in prior study.³⁰ All the statistical analyses were carried out using SPSS V26.0.

Results and discussion

Mass concentration

On March 28 and March 29, 2015, air masses originated from northern direction of Beijing dominated the sampling location, which transported dust particles from Mongolia and Inner Mongolia Plateau over the sampling site (Fig. 2A). The mass concentrations of PM₁₀ and PM_{2.5} at S₁ increased to higher than 250 and 75 $\mu\text{g m}^{-3}$ due to inputs of the dust storm, respectively (Fig. 3A and B).

As shown in Fig. 3B, the mass concentrations of PM_{2.5} at sites S₂, S₃ and S₄ on the individual dates (March 16, March 17, April 9, April 15, April 17, November 12, 13, 14) were observed to be higher than 75 $\mu\text{g m}^{-3}$. Daily atmospheric visibilities for these dates obtained from Beijing Meteorological service were all lower than 10 km. Thus, the weather for these days was haze days (Table S1[†]). Local air masses dominated the sampling location during these individual dates. For these haze days, the average mass concentrations of PM₁₀ at S₂, S₃ and S₄ were 215 $\mu\text{g m}^{-3}$, 231 $\mu\text{g m}^{-3}$ and 214 $\mu\text{g m}^{-3}$, respectively (Fig. 3A). For PM_{2.5}, the mean levels at S₂, S₃ and S₄ were 189 $\mu\text{g m}^{-3}$, 125 $\mu\text{g m}^{-3}$, and 148 $\mu\text{g m}^{-3}$, respectively (Fig. 3B).

Chemical components

As shown in Fig. 3A and B, the total concentrations of secondary inorganic ions (NO₃⁻, SO₄²⁻ and NH₄⁺) were the largest contributors to PM_{2.5} and PM₁₀ mass across all the samples, which accounted for about 20–40% of PM_{2.5} mass and PM₁₀ mass, respectively. High fractions of secondary ions (~20–40%) contributing to PM mass concentration in haze samples were observed in this study, which is consistent with several field studies in Beijing,^{5,24,31} suggesting secondary photochemical reactions were enhanced during the haze events in Beijing.²³ Other ions including Cl⁻, Na⁺, K⁺, Mg²⁻, Ca²⁺ and F⁻ contributed a small fraction to PM_{2.5} mass and PM₁₀ mass, which were in the range of 1–5% of PM_{2.5} mass and PM₁₀ mass, respectively. The concentrations of Ca²⁺ on dust PM samples were 1–2 times greater than that in haze seasons, which could be attributed to

the increases of crystal metals (*e.g.*, Ca) during dust storm events.⁸

Levels of metals including As, Cr, Cu, Ni, Pb, Mn, and Ni in all measured PM₁₀ and PM_{2.5} samples ranged from 0.005–0.03 $\mu\text{g m}^{-3}$ and 0.004–0.02 $\mu\text{g m}^{-3}$, respectively (Fig. 3B). The total concentrations of metals accounted for ~5% of PM₁₀ mass and ~3% of PM_{2.5} mass, respectively. There were no significant differences observed in the levels of total metals in PM samples on individual date (Fig. 3A and B). The concentrations of OC in PM₁₀ and PM_{2.5} samples were in the range of 15.9–26.9 $\mu\text{g m}^{-3}$ and 18.4–30.9 $\mu\text{g m}^{-3}$, while the levels of EC ranged from 1.1–8.3 $\mu\text{g m}^{-3}$ and 2.3–9.8 $\mu\text{g m}^{-3}$, respectively (Fig. 3A and B). The OC/EC ratios greater than 3 indicated higher photochemical secondary reactions occurred in all samples collected from the pollution days. The sum of PAHs in PM₁₀ and PM_{2.5} were in the range of 50–250 ng m^{-3} and 50–200 ng m^{-3} , respectively. BaP was observed to be the dominant species in all the PM samples, ranging from 4–36 ng m^{-3} (Fig. 4A and B). The national limit of

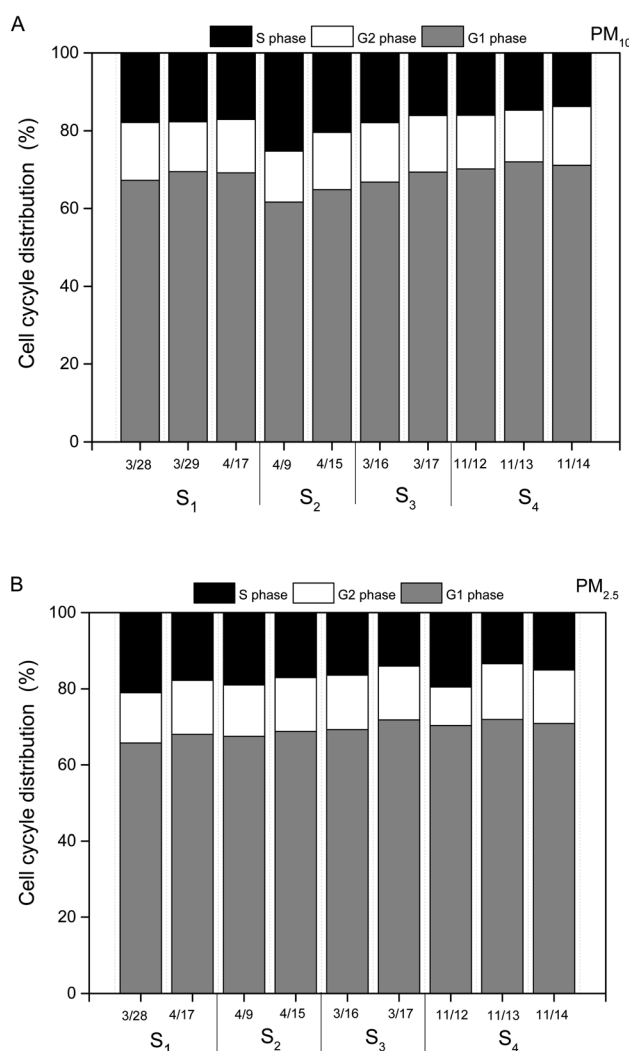


Fig. 6 Cell cycle distribution in human bronchial epithelial cells with mass normalized PM water extracts ($1 \mu\text{g mL}^{-1}$) after 24 h exposure. (A) Cells with mass normalized PM₁₀ water extracts ($1 \mu\text{g mL}^{-1}$). (B) Cells with mass normalized PM_{2.5} water extracts ($1 \mu\text{g mL}^{-1}$).



daily BaP in outdoor air is 2.5 ng m^{-3} in China.³² BaP in all PM samples were observed to be higher than the national limit of BaP, posing greater health risk to the public.

Cell survival rate

Fig. 5B and C presented the optical micrographs of HBE cells treated with PM₁₀ water extracts ($1 \mu\text{g mL}^{-1}$) and PM_{2.5} water extracts ($1 \mu\text{g mL}^{-1}$). Compared with HBE cells without PM water extracts (Fig. 5A), higher fractions of cell were found to exhibit apoptosis. The survival rates of HBE cells exposed to PM₁₀ water extracts were in the range of 60–90%, which were considerably higher than those exposed to PM_{2.5} water extracts (~40–70%) (Fig. 5D and E). This finding supports the previous studies that the size of particle is a factor to induce the toxicity to the cells.^{1,14,20} There were no significant differences in survival rates of the cells exposed to PM₁₀ or PM_{2.5} collected from different individual dates.

Cell cycle arrest

Cells exposed to PM water extracts could be the result of apoptosis or cell cycle arrest or a combination of these.¹⁹ Thus,

we introduced the ambient PM samples into HBE cells for understanding the key factor resulting in cell cycle arrest.²⁰ As shown in Fig. 6A and B, water extracts of PM ($1 \mu\text{g mL}^{-1}$) could lead to clear cell cycle distribution in different phases. For all the PM₁₀ samples, ~65% in the percentage of cells in G0/G1 phase, ~15% in the percentage of cells in G1/G2 phase and ~20% in the percentage of cells in G2/S phase were observed. Similar cell cycle distributions were found in the HBE cells exposed to PM_{2.5} water extracts (65% of cells in G0/G1 phase, 15% of cells in G1/G2 phase, 20% of cells in G2/S phase). The results indicated that the main toxicity mechanism induced by PM water extracts on HBE cells was G0/G1 phase arrest. Prior studies showed that cells arrest in G0/G1 could lead to DNA repair.¹⁹ No significant differences in cell cycle distributions of HBE exposed to PM₁₀ or PM_{2.5} samples across individual dates were found.

Chemical compositions and cell cycle arrest

We did not observe significant associations between mass concentrations of PM₁₀ or PM_{2.5} with cell survival rate or cell cycle arrest in HBE cells. Our result was in agreement with the

Table 1 Spearman correlation (*R*) between cell survival rate and cell cycle distribution with PM₁₀ mass and chemical components. Bold values indicate $\rho \geq 0.50$ or $\rho \leq -0.50^a$

Item	Cell survival rate	Adjusted <i>p</i>	G1	Adjusted <i>p</i>	G2	Adjusted <i>p</i>	S	Adjusted <i>p</i>
Mass	0.281	0.13	-0.134	0.11	-0.216	0.11	0.115	0.14
Cl ⁻	0.162	0.11	0.132	0.17	-0.479	0.07	0.063	0.19
NO ₃ ⁻	0.425	0.12	-0.221	0.18	-0.245	0.08	0.350	0.17
SO ₄ ²⁻	0.465	0.14	-0.174	0.09	-0.610	0.06	0.427	0.15
Na ⁺	0.362	0.15	-0.536	0.13	0.280	0.13	0.354	0.16
NH ₄ ⁺	-0.239	0.12	0.444	0.14	0.030	0.14	-0.368	0.10
K ⁺	0.194	0.11	0.190	0.13	-0.346	0.13	-0.038	0.13
Mg ²⁺	0.329	0.12	-0.322	0.13	-0.127	0.13	0.277	0.20
Ca ²⁺	0.088	0.14	-0.045	0.07	-0.118	0.07	0.020	0.14
OC	0.020	0.13	-0.343	0.18	-0.048	0.08	0.256	0.12
EC	-0.414	0.12	0.464	0.08	0.055	0.08	-0.409	0.11
Nap	-0.642	0.13	0.850**	0.03	-0.080	0.10	-0.932**	0.02
AcPy	-0.111	0.08	-0.555	0.10	0.748*	0.02	0.305	0.15
Acp	0.438	0.10	-0.674*	0.02	0.205	0.10	0.676*	0.01
Flu	0.451	0.11	-0.685*	0.02	0.177	0.08	0.702*	0.04
PA	-0.086	0.14	-0.383	0.11	0.545	0.09	0.197	0.12
Ant	-0.529	0.15	0.293	0.17	0.042	0.08	-0.356	0.11
FL	-0.660	0.17	0.295	0.08	0.185	0.16	-0.418	0.15
BaA	-0.768*	0.02	0.618	0.06	0.104	0.15	-0.752*	0.04
Pyr	-0.703*	0.02	0.606	0.13	0.155	0.11	-0.760*	0.03
BbF	-0.693*	0.03	0.641	0.14	0.115	0.17	-0.783*	0.02
BkF	-0.707*	0.02	0.701*	0.03	-0.012	0.18	-0.795*	0.02
BaP	-0.763*	0.02	0.655	0.11	0.028	0.06	-0.760*	0.02
IND	-0.685*	0.02	0.650	0.11	0.082	0.13	-0.779*	0.04
DBA	-0.691*	0.03	0.623	0.10	0.084	0.14	-0.749*	0.03
BghiP	-0.715*	0.02	0.644	0.08	0.089	0.13	-0.774*	0.04
As	0.289	0.15	0.083	0.11	-0.705*	0.03	0.166	0.14
Cr	0.083	0.12	0.046	0.11	-0.296	0.17	-0.048	0.12
Cu	0.182	0.15	-0.342	0.11	-0.255	0.18	0.345	0.11
Ni	-0.494	0.16	0.655*	0.03	-0.142	0.18	-0.529	0.12
Pb	0.515	0.15	-0.291	0.11	-0.727*	0.02	0.497	0.15
Mn	0.523	0.12	-0.319	0.17	-0.676*	0.03	0.487	0.11
Zn	0.450	0.13	-0.373	0.108	-0.528	0.10	0.477	0.10

^a **p* < 0.05, ***p* < 0.01.



Table 2 Spearman correlation (R) between cell survival rate and cell cycle distribution with PM_{2.5} mass and chemical components. Bold values indicate $\rho \geq 0.50$ or $\rho \leq -0.50^a$

Item	Cell survival rate	Adjusted p	G1	Adjusted p	G2	Adjusted p	S	Adjusted p
Mass	0.281	0.19	-0.134	0.15	-0.216	0.16	0.115	0.20
Cl ⁻	-0.340	0.16	0.222	0.17	-0.214	0.17	-0.067	0.20
NO ₃ ⁻	-0.207	0.11	0.051	0.07	0.041	0.14	-0.063	0.22
SO ₄ ²⁻	0.151	0.15	0.125	0.18	-0.162	0.18	-0.016	0.13
Na ⁺	-0.281	0.19	-0.174	0.14	0.229	0.16	0.020	0.15
NH ₄ ⁺	-0.187	0.12	0.578	0.20	-0.171	0.11	-0.377	0.12
K ⁺	0.138	0.09	-0.117	0.13	-0.291	0.18	0.248	0.19
Mg ²⁺	-0.377	0.11	-0.509	0.10	0.229	0.16	0.291	0.14
Ca ²⁺	-0.313	0.08	-0.158	0.04	0.291	0.12	-0.025	0.16
OC	-0.450	0.14	-0.278	0.02	-0.309	0.12	0.388	0.14
EC	-0.253	0.18	0.843**	0.02	-0.335	0.16	-0.505	0.14
Nap	0.641*	0.04	0.042	0.03	-0.229	0.15	0.087	0.12
AcPy	0.159	0.17	-0.612*	0.02	-0.049	0.14	0.521*	0.02
Acp	-0.445	0.11	-0.618*	0.02	0.106	0.13	0.445	0.19
Flu	-0.426	0.10	-0.591*	0.03	0.135	0.15	0.407	0.08
PA	-0.418	0.11	0.182	0.08	0.089	0.11	-0.194	0.08
Ant	0.033	0.14	-0.511*	0.03	-0.346	0.13	0.596*	0.02
FL	-0.187	0.10	0.592*	0.02	-0.323	0.13	-0.309	0.11
BaA	-0.206	0.16	0.605*	0.03	-0.385	0.16	-0.286	0.24
Pyr	-0.117	0.19	0.704*	0.01	-0.479	0.15	-0.316	0.10
BbF	-0.087	0.16	0.712*	0.02	-0.438	0.14	-0.345	0.09
BkF	-0.005	0.11	0.696*	0.02	-0.379	0.18	-0.363	0.12
BaP	-0.082	0.15	0.563*	0.04	-0.506	0.16	-0.188	0.13
IND	-0.129	0.19	0.667*	0.03	-0.527	0.15	-0.262	0.16
DBA	-0.047	0.13	0.611*	0.03	-0.499	0.18	-0.231	0.11
BghiP	-0.050	0.19	0.653*	0.02	-0.496	0.16	-0.266	0.12
As	0.543	0.11	-0.041	0.04	-0.142	0.12	0.121	0.14
Cr	-0.652	0.08	0.220	0.02	-0.286	0.12	0.018	0.12
Cu	-0.372	0.14	-0.076	0.06	0.239	0.16	-0.097	0.12
Ni	-0.251	0.18	0.567	0.05	-0.375	0.15	-0.185	0.04
Pb	0.019	0.14	-0.391	0.09	0.022	0.14	0.279	0.12
Mn	0.145	0.17	-0.532	0.08	-0.086	0.13	0.455	0.17
Zn	-0.245	0.11	-0.458	0.09	0.102	0.15	0.278	0.19

^a * $p < 0.05$, ** $p < 0.01$.

prior finding that mass concentration is not a good indicator for assessing health effects related to the exposures of ambient PM pollution^{6,12} (Tables 1 and 2).

For PM₁₀ samples, the highest association between cell survival rate and chemical components were BaA ($\rho = 0.768$, $p = 0.02$), followed by BaP ($\rho = 0.763$, $p = 0.02$), BghiP ($\rho = 0.715$, $p = 0.02$), BkF ($\rho = 0.707$, $p = 0.02$), Pyr ($\rho = 0.703$, $p = 0.02$), BbF ($\rho = 0.693$, $p = 0.03$), DBA ($\rho = 0.691$, $p = 0.03$), IND ($\rho = 0.685$, $p = 0.02$). Individual chemical components including Nap ($\rho = 0.850$, $p = 0.03$), Acp ($\rho = 0.674$, $p = 0.02$), Flu ($\rho = 0.685$, $p = 0.02$), BkF ($\rho = 0.701$, $p = 0.03$) and Ni ($\rho = 0.655$, $p = 0.03$) were significantly associated with the percentage of cells in G0/G1 phase. Naphthalene, As and Ni were strongly correlated with the percentage of cells in G1/G2 phase, while some PAH compounds (*i.e.*, Nap, AcPy, Flu, BaA, Pyr, BbF, BkF, BaA, IND, DBA, BghiP) were strongly correlated with the percentage of cells in G0/S phase ($\rho = 0.70$ – 0.90 , $p = 0.01$ – 0.04) (Table 1).

Similarly, individual chemical species (Nap) of PAHs in PM_{2.5} showed significant correlation with cell survival rate (ρ , 0.641). The percentage of cells in G0/G1 phase was highly associated with PM_{2.5} chemical species including EC (ρ , 0.843) and PAHs

(*i.e.*, AcPy, Acp, Flu, FL, BaA, Pyr, BbF, BkF, BaP, IND, DBA, BghiP) ($\rho = 0.50$ – 0.85 , $p = 0.02$ – 0.04). The percentage of cells in G2/S phase was significantly related with AcPy ($\rho = 0.521$, $p = 0.02$) and Acp ($\rho = 0.596$, $p = 0.02$) in PM_{2.5} (Table 2).

Previous studies have presented evidence that PAHs exposures could lead to cell cycle arrest at G0/G1 phase.^{15,17} Our field study supports this evidence. In addition, our study found EC and some metals (*e.g.*, Ni, As) were also correlated with cell cycle arrest at G0/G1 phase or G1/G2 phase. These chemical compounds (*i.e.* EC, As, Ni, PAHs) appeared to be released from fuel combustion.⁵

Since the chemical composition of the PM in the cell culture was water-soluble, our study has several limitations including the fact that an inability to account for water insoluble substances responsible for cell cycle arrest in HBE cells. Our finding suggests a potential role of co-pollutants in altering cell cycle in HBE cells. Although the mechanisms of how these chemical compounds influence cell cycle are unclear and needed to be further studied, the results of our study demonstrate the roles of specific chemical compounds in altering cell cycle across different PM sample types. Our study provides



further motivation to assess the mechanism of the specific chemical components of PM in mediating cell cycles in HBE cells.

Conclusion

Ambient PM₁₀ and PM_{2.5} of dust storm and haze samples were collected. The mass concentrations of PM₁₀ and PM_{2.5} were in the range of 120–350 µg m⁻³ and 80–250 µg m⁻³, respectively. Secondary ions including nitrate, sulfate and ammonium contributed the greatest fraction to total PM mass (~20–40%), followed by OC (~8–15%), primary ions (~8–12%), EC (~2–5%) and metals (~1–2%). The total concentrations of PAHs in PM₁₀ and PM_{2.5} ranged as 40–250 ng m⁻³ and 50–150 ng m⁻³, respectively. No significant differences in chemical components of PM across individual samples were observed during the sampling period. The survival rate of HBE cells induced by PM₁₀ water extracts were lower than that by PM_{2.5} water extracts. The individual chemical components (PAHs, As, Ni, EC), other than total mass, were highly associated with the distribution of cell cycles in HBE cells. This study provides targeted compounds for reductions to protect public health during high air pollution periods in Beijing.

Conflicts of interest

There are no conflict to declare.

Acknowledgements

This research was supported by the National Nature Science Foundation of China (41475133). We would like to appreciate the comments from two anonymous reviewers for improving the quality of the manuscript.

References

- 1 IARC, *Outdoor air pollution a leading environmental cause of cancer deaths*, 2013.
- 2 R. Burnett, H. Chen, M. Szyszkowicz, N. Fann, B. Hubbell, C. A. Pope, J. S. Apte, M. Brauer, A. Cohen, S. Weichenthal, J. Coggins, Q. Di, B. Brunekreef, J. Frostad, S. S. Lim, H. Kan, K. D. Walker, G. D. Thurston, R. B. Hayes, C. C. Lim, M. C. Turner, M. Jerrett, D. Krewski, S. M. Gapstur, W. R. Diver, B. Ostro, D. Goldberg, D. L. Crouse, R. V. Martin, P. Peters, L. Pinault, M. Tjepkema, A. van Donkelaar, P. J. Villeneuve, A. B. Miller, P. Yin, M. Zhou, L. Wang, N. A. H. Janssen, M. Marra, R. W. Atkinson, H. Tsang, T. Quoc Thach, J. B. Cannon, R. T. Allen, J. E. Hart, F. Laden, G. Cesaroni, F. Forastiere, G. Weinmayr, A. Jaensch, G. Nagel, H. Concin and J. V. Spadaro, *Proc. Natl. Acad. Sci. U. S. A.*, 2018, **115**, 9592.
- 3 R. E. Arku, A. Birch, M. Shupler, S. Yusuf, P. Hystad and M. Brauer, *Environ. Int.*, 2018, **114**, 307–317.
- 4 F. Tian, J. Qi, L. Wang, P. Yin, Z. Qian, Z. Ruan, J. Liu, Y. Liu, S. E. McMillin, C. Wang, H. Lin and M. Zhou, *Environ. Int.*, 2020, **145**, 106096.
- 5 Q. Liu, J. Baumgartner, Y. Zhang and J. J. Schauer, *Atmos. Environ.*, 2016, **126**, 28–35.
- 6 Q. Liu, J. Baumgartner, Y. Zhang, Y. Liu, Y. Sun and M. Zhang, *Environ. Sci. Technol.*, 2014, **48**, 12920–12929.
- 7 Q. Liu, J. Baumgartner and J. J. Schauer, *Environ. Sci. Technol.*, 2019, **53**, 9845–9854.
- 8 Q. Liu, Y. Liu, J. Yin, M. Zhang and T. Zhang, *Atmos. Environ.*, 2014, **91**, 85–94.
- 9 W. Liu, Y. Xu, W. Liu, Q. Liu, S. Yu, Y. Liu, X. Wang and S. Tao, *Environ. Pollut.*, 2018, **236**, 514–528.
- 10 Z. Lu, Q. Liu, Y. Xiong, F. Huang, J. Zhou and J. J. Schauer, *Environ. Pollut.*, 2018, **238**, 39–51.
- 11 C. Brehmer, A. Lai, S. Clark, M. Shan, K. Ni, M. Ezzati, X. Yang, J. Baumgartner, J. J. Schauer and E. Carter, *Environ. Sci. Technol.*, 2019, **53**, 2788–2798.
- 12 Q. Liu, Z. Lu, Y. Xiong, F. Huang, J. Zhou and J. J. Schauer, *Sci. Total Environ.*, 2020, **701**, 134844.
- 13 R. J. Delfino, N. Staimer, T. Tjoa, M. Arhami, A. Polidori, D. L. Gillen, S. C. George, M. M. Shafer, J. J. Schauer and C. Sioutas, *Epidemiology*, 2010, **21**, 892–902.
- 14 T. Xiao, M. Ling, H. Xu, F. Luo, J. Xue, C. Chen, J. Bai, Q. Zhang, Y. Wang, Q. Bian and Q. Liu, *Toxicol. Appl. Pharmacol.*, 2019, **377**, 114616.
- 15 T. J. Ronkko, M. R. Hirvonen, M. S. Happonen, T. Ihanntola, H. Hakkarainen, M. V. Martikainen, C. Gu, Q. Wang, J. Jokiniemi, M. Komppula and P. I. Jalava, *Environ. Res.*, 2021, **192**, 110382.
- 16 Y. Xu, J. Wu, X. Peng, T. Yang, M. Liu, L. Chen, X. Dai, Z. Wang, C. Yang, B. Yan and Y. Jiang, *Toxicol. Lett.*, 2017, **276**, 1–10.
- 17 Z. Qin, H. Hou, F. Fu, J. Wu, B. Han, W. Yang, L. Zhang, J. Cao, X. Jin, S. Cheng, Z. Yang, M. Zhang, X. Lan, T. Yao, Q. Dong, S. Wu, J. Zhang, Z. Xu, Y. Li and Y. Chen, *Reprod. Toxicol.*, 2017, **74**, 10–22.
- 18 T. Xiao, M. Ling, H. Xu, F. Luo, J. Xue, C. Chen, J. Bai, Q. Zhang, Y. Wang, Q. Bian and Q. Liu, *Toxicol. Appl. Pharmacol.*, 2019, **377**, 114616.
- 19 Y. Fu, Y. Niu, B. Pan, Y. Liu, B. Zhang, X. Li, A. Yang, J. Nie, R. Wang and J. Yang, *Chemosphere*, 2019, **224**, 48–57.
- 20 E. Reyes-Zarate, Y. Sanchez-Perez, M. C. Gutierrez-Ruiz, Y. I. Chirino, A. R. Osornio-Vargas, R. Morales-Barcenas, V. Souza-Arroyo and C. M. Garcia-Cuellar, *Environ. Pollut.*, 2016, **214**, 646–656.
- 21 W. Cai and P. Ye, *J. Cleaner Prod.*, 2020, **276**, 124105.
- 22 B. Tilt, *Environ. Sci. Policy*, 2019, **92**, 275–280.
- 23 X. Li, L. Jiang, Y. Bai, Y. Yang, S. Liu, X. Chen, J. Xu, Y. Liu, Y. Wang, X. Guo, Y. Wang and G. Wang, *Atmos. Res.*, 2019, **218**, 25–33.
- 24 Z. Wang, W. Hu, H. Niu, W. Hu, Y. Wu, L. Wu, L. Ren, J. Deng, S. Guo, Z. Wu, D. Zhang, P. Fu and M. Hu, *Sci. Total Environ.*, 2020, **762**, 143081.
- 25 F. Bilo, L. Borgese, A. Wambui, A. Assi, A. Zacco, S. Federici, D. M. Eichert, K. Tsuji, R. G. Lucchini, D. Placidi, E. Bontempi and L. E. Depero, *J. Aerosol Sci.*, 2018, **122**, 1–10.



Paper

- 26 N. T. H. Nga, T. T. B. Ngoc, N. T. M. Trinh, T. L. Thuoc and D. T. P. Thao, *Anal. Biochem.*, 2020, **610**, 113937.
- 27 Y. Xu, J. Wu, X. Peng, T. Yang, M. Liu, L. Chen, X. Dai, Z. Wang, C. Yang, B. Yan and Y. Jiang, *Toxicol. Lett.*, 2017, **276**, 1–10.
- 28 G. Rolph, A. Stein and B. Stunder, *Environ. Modell. Softw.*, 2017, **95**, 210–228.
- 29 J. R. Stevens, A. A. Masud and A. Suyundikov, *PLoS One*, 2017, **12**, e0176124.
- 30 A. H. Al Hanai, D. C. Antkiewicz, J. D. C. Hemming, M. M. Shafer, A. M. Lai, M. Arhami, V. Hosseini and J. J. Schauer, *Environ. Int.*, 2019, **123**, 417–427.
- 31 L. Xu, F. Duan, K. He, Y. Ma, L. Zhu, Y. Zheng, T. Huang, T. Kimoto, T. Ma, H. Li, S. Ye, S. Yang, Z. Sun and B. Xu, *Environ. Pollut.*, 2017, **227**, 296–305.
- 32 Ministry of Environmental Protection of the People's Republic of China, *Ambient air quality standards*, 2012.

